

# CoT-Saliency: Unified Chain-of-Thought Reasoning for Heterogeneous Saliency Tasks

Long Li

Northwestern Polytechnical University

Ziyang Luo

Northwestern Polytechnical University

Dingwen Zhang

Northwestern Polytechnical University

Shuichen Ji

Northwestern Polytechnical University

Nian Liu\*

Northwestern Polytechnical University

Junwei Han

Northwestern Polytechnical University

## Abstract

We present the first unified framework that jointly handles three operationally heterogeneous saliency tasks, i.e., SOD, CoSOD, and SIS, by casting each as a Chain-of-Thought (CoT) reasoning process in a Vision-Language Model (VLM) to bridge task heterogeneity. CoT training follows a two-stage paradigm: Supervised Fine-Tuning (SFT) and Reinforcement Learning (RL). To enhance CoT quality in RL, we propose Confidence-Guided Policy Optimization (CGPO), a lightweight single-sample algorithm that leverages the discrepancy between reward and model confidence as a per-sample advantage signal. This design naturally focuses updates on informative responses while eliminating group sampling, thereby addressing GRPO’s key limitations: confidence-agnostic learning, signal dilution, and prohibitive computational overhead. We also introduce an “output-to-reasoning” strategy to construct high-fidelity SFT data that ensures logical consistency with ground-truth masks. Experiments show our model matches or outperforms specialized SOTA methods and strong closed-source VLMs across all tasks, especially achieving an S-measure of 0.899 on CoCA for CoSOD, surpassing the prior best by 8.0 percentage points, despite using far less training data.

## 1. Introduction

Recently, Multimodal Large Language Models (MLLMs) have demonstrated remarkable capabilities in complex reasoning tasks. By leveraging structured reasoning mechanisms like Chain-of-Thought (CoT), these models effec-

tively integrate visual input with linguistic logic, achieving strong performance in visual question answering, image captioning, and referring expression comprehension, and so on. Although many MLLMs like GPT-4o, Qwen2.5-VL, and Claude Sonnet exhibit impressive zero-shot generalization across a wide range of domains, they are not universally component. Especially in saliency detection tasks, these powerful models perform surprisingly poorly. This is due to MLLMs lack of fine-grained perceptual reasoning grounded in saliency principles, such as contrast, center bias, object completeness, and inter-instance distinctiveness.

This paper aims to fill the gap in the reasoning ability of MLLMs in the field of saliency detection. Saliency detection comprises a variety of subtasks, among which Salient Object Detection (SOD), Co-salient Object Detection (CoSOD), and Salient Instance Segmentation (SIS) are three representative and operationally heterogeneous formulations. SOD identifies region-level prominent objects in a single image. CoSOD seeks a shared semantic category across a group of images. SIS further disambiguates individual instances within a single image. In order to comprehensively address saliency detection, we struggle to unify these three representative tasks into a single MLLM framework.

Recent MLLM-based segmentation frameworks have made impressive strides, but none are well-suited for unifying these three saliency tasks. LISA and SegLLM rely on special tokens (e.g.,  $i\text{SEG}_i$ ) to trigger mask generation, but their architectures assume a fixed output format and cannot distinguish between region-level, instance-level, or semantic-category outputs. HyperSeg unifies diverse segmentation tasks but relies on user-specified prompts or cat-

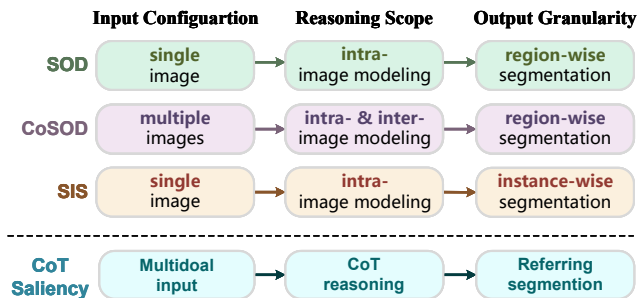


Figure 1. **Task heterogeneity across SOD, CoSOD, and SIS.** These three tasks differ fundamentally in input configuration, output granularity, and reasoning scope. Our CoT-Saliency framework unifies them via a shared CoT interface.

egory labels, and thus cannot perform autonomous saliency reasoning where the salient content must be discovered without prior semantic guidance. Other approaches, such as ThinkFirst, which uses GPT-4o’s CoT to guide a frozen segmenter, or LENS, which extracts keypoints from MLLM attention maps, either depend on proprietary APIs or lack the structured semantics needed to differentiate CoSOD’s shared category from SIS’s disambiguated instances.

Salient Object Detection (SOD) [26, 27, 29, 47, 54, 57, 63] aims to identify and segment the most visually prominent regions in a single image. Co-salient Object Detection (CoSOD) [23, 24, 40, 53, 58, 62] extends this to a group of related images, seeking common salient objects across all of them. Salient Instance Segmentation (SIS) [12, 35, 49] further refines SOD by distinguishing individual salient instances. While task-specific models have achieved strong performance, a *unified framework* that jointly handles these three tasks remains missing.

Such a unified model is highly desirable: it eliminates redundant designs, improves data efficiency through shared representations, and simplifies deployment and extension to new saliency tasks [15, 19].

However, unifying these tasks is fundamentally challenging due to their operational heterogeneity. As shown in Figure 1, they differ in three key aspects: (1) *input configuration*: SOD and SIS take a single image, while CoSOD requires a group of images; (2) *output granularity*: SOD and CoSOD produce region-level masks, whereas SIS segments individual instances; and (3) *reasoning scope*: SOD uses only intra-image cues, CoSOD requires cross-image consensus, and SIS performs instance-level disambiguation within a single image.

To address this, we propose **CoT-Saliency**, the first framework that unifies these three operationally heterogeneous saliency tasks by casting each as a Chain-of-Thought (CoT) reasoning process [48] within a Vision-Language Model (VLM) [3]. As illustrated in Figure 1, using task-specific instructions, the VLM generates structured

CoT outputs that are parsed and fed into a frozen referring segmentation model [59] to produce task-appropriate masks, thereby bridging task heterogeneity through a shared language-mediated pipeline.

To enhance CoT reasoning quality, we adopt the standard two-stage training paradigm: Supervised Fine-Tuning (SFT) followed by Reinforcement Learning (RL) [13]. GRPO [36] is a widely used RL algorithm, but it has three critical limitations: (1) *confidence-agnostic*: it ignores the model’s own prediction confidence, wasting computation on uninformative responses, *i.e.*, well-learned (high reward & high confidence) and inherently unreliable (low reward & low confidence), while failing to focus on the most informative ones, *i.e.*, under-explored correct responses (high reward & low confidence) and overconfident errors (low reward & high confidence); (2) *signal dilution*: the shared group-mean baseline causes well-learned responses to dilute the rewards for correct but under-explored ones, and unreliable responses to weaken the penalties for confidently generated errors; (3) *prohibitive overhead*: it incurs high computational cost from both (i) generating multiple parallel CoT traces per input and (ii) computing a KL-divergence penalty against a frozen reference model, resulting in substantially higher memory usage and longer training time per step.

To address these limitations, we propose Confidence-Guided Policy Optimization (CGPO), a lightweight single-sample reinforcement learning algorithm that jointly resolves all three issues. First, inspired by calibration principles in Bayesian reasoning [7, 32], CGPO treats the model’s prediction confidence as a belief over correctness and reward as observational evidence, constructing a per-sample advantage signal as their discrepancy. This design naturally focuses updates on informative responses, where belief (confidence) and evidence (reward) disagree, and eliminates the need for group-based sampling, thereby avoiding signal dilution and removing the requirement for multiple parallel CoT traces per input. Second, to further reduce computational overhead, CGPO removes the need for a frozen reference model by replacing KL-divergence regularization with Interleaved SFT Regularization (ISR), which stabilizes training through periodic SFT steps.

We also propose an “output-to-reasoning” strategy for SFT data construction: instead of asking a closed-source world model [2] to generate ground-truth CoT from scratch [31, 50], we provide ground-truth masks and prompt it to explain saliency, yielding high-fidelity CoT sequences that are logically consistent with the segmentation labels.

In summary, our main contributions are as follows:

- We present the first unified framework that jointly handles three operationally heterogeneous saliency tasks, *i.e.*, SOD, CoSOD, and SIS, by casting each as a CoT reasoning process within a VLM.

- We propose CGPO, a lightweight single-sample RL algorithm that utilizes reward-confidence discrepancy as a per-sample advantage signal, replaces KL-divergence with ISR, and requires only one CoT trace per input.
- We propose an “output-to-reasoning” SFT strategy that ensures CoT–output alignment and surpasses the data-generation world model.

## 2. Related Work

### 2.1. Saliency Detection

**Salient Object Detection (SOD).** SOD segments the most visually prominent regions in an image. Early deep learning methods like PiCANet [26] used contextual attention to fuse global and local cues, while label decoupling [47] improved boundary sharpness. Later works enhanced object completeness via part-whole modeling [29, 63]. Recently, Transformer-based models have dominated, *e.g.*, VST [27] introduced a pure Vision Transformer for SOD, while others integrated generative priors [57] or self-refinement mechanisms [54].

**Co-Salient Object Detection (CoSOD).** CoSOD identifies common salient objects across a group of images [11, 38], requiring cross-image consensus. Recent methods model this via diverse strategies: CADc [58] uses cross-image attention; DCFM [53] builds democratic prototypes; GCoNet+ [62] enforces group collaboration; DMT+ [24] mines co-salient and background regions; CONDA [23] refines inter-image associations; and VCP [40] adapts foundation models via visual consensus prompts with minimal parameter tuning.

**Salient Instance Segmentation (SIS).** SIS extends SOD by segmenting salient objects at the instance level in a category-agnostic manner [12, 34]. Early multi-stage pipelines suffered from error propagation [21], while later end-to-end models like S4Net [12] and RDPNet [49] improved robustness. Recent Transformer-based approaches such as OQTR [35] use query-driven, anchor-free detection, eliminating hand-crafted components like NMS [45].

Although strong task-specific models exist for SOD, CoSOD, and SIS, no unified framework handles these operationally heterogeneous tasks within a single architecture. We bridge this gap to jointly address all three tasks via a common CoT reasoning paradigm.

### 2.2. Unified Salient Detection Framework

Existing unified segmentation frameworks fall into two paradigms: (1) query-based models like Mask2Former [4], which unify category-specified tasks, *i.e.*, semantic, instance, and panoptic segmentation, but it requires a closed vocabulary; and (2) promptable models like SAM [19], which support flexible zero-shot segmentation but lack intrinsic saliency awareness. Within saliency detection, recent

unified methods, *i.e.*, UniSOD [41], Samba [14], and VS-Code [30], only handle *operationally homogeneous* tasks: all take a single image (or pair) and output a binary mask.

In contrast, our framework is the first to unify *operationally heterogeneous* saliency tasks: SOD (single image), CoSOD (image group), and SIS (category-agnostic instance separation), which differ fundamentally in input configuration, output granularity, and reasoning scope.

### 2.3. Vision-Language Models for Segmentation

Recent works explore VLMs for segmentation. LISA [20] links VLMs to segmentation decoders via a <SEG> token but lacks explicit CoT. ThinkFirst [17] uses GPT-4o’s CoT to guide a frozen segmenter but depends on proprietary models and is not end-to-end trainable. Seg-Zero [28] and PIXELTHINK [44] train CoT with RL, while RESAnything [43] adopts a zero-shot approach.

In contrast, we cast all saliency tasks as CoT reasoning in a VLM, which outputs structured language prompts for a frozen referring segmenter. This yields a unified, end-to-end, task-aware framework. To enhance CoT quality, we propose CGPO, a lightweight RL algorithm that overcomes GRPO’s key limitations: confidence-agnostic learning, signal dilution, and prohibitive computational overhead.

## 3. Proposed Method

### 3.1. Framework Construction

**Overview.** As shown in Figure 2, given a visual input  $I$  and a task instruction  $\tau \in \{\tau^{SOD}, \tau^{CoSOD}, \tau^{SIS}\}$ , the VLM (Qwen2.5-VL [3]) generates a structured CoT response, which is parsed and fed to a frozen referring segmenter (EVF-SAM [59]), denoted by  $\mathcal{S}$ , to produce the final mask(s).

**Input format.** The visual input  $I$  and instruction  $\tau$  are task-specific:

- **SOD/SIS:**  $I = \{x^{SOD}\}/\{x^{SIS}\}$  (single image);  $\tau^{SOD}$  prompts step-by-step reasoning to describe visually prominent regions, while  $\tau^{SIS}$  requires enumerating all distinct instances with disambiguating attributes (*e.g.*, location, color).
- **CoSOD:**  $I = \{x_k^{CoSOD}\}_{k=1}^K$  (a group of  $K$  images);  $\tau^{CoSOD}$  guides the model to identify a shared semantic category across images.

All task instruction templates are provided in Figure 4.

**Canonical CoT format.** The VLM output follows:

$$\langle \text{think} \rangle \mathcal{R}_{\text{CoT}} \langle \text{/think} \rangle \langle \text{answer} \rangle \mathcal{E} \langle \text{/answer} \rangle, \quad (1)$$

where  $\mathcal{R}_{\text{CoT}}$  is a three-step reasoning chain (scene/object identification  $\rightarrow$  task-specific analysis  $\rightarrow$  conclusion), and  $\mathcal{E}$  is the referring expression that encodes task-specific language prompts for the downstream segmenter. It can be

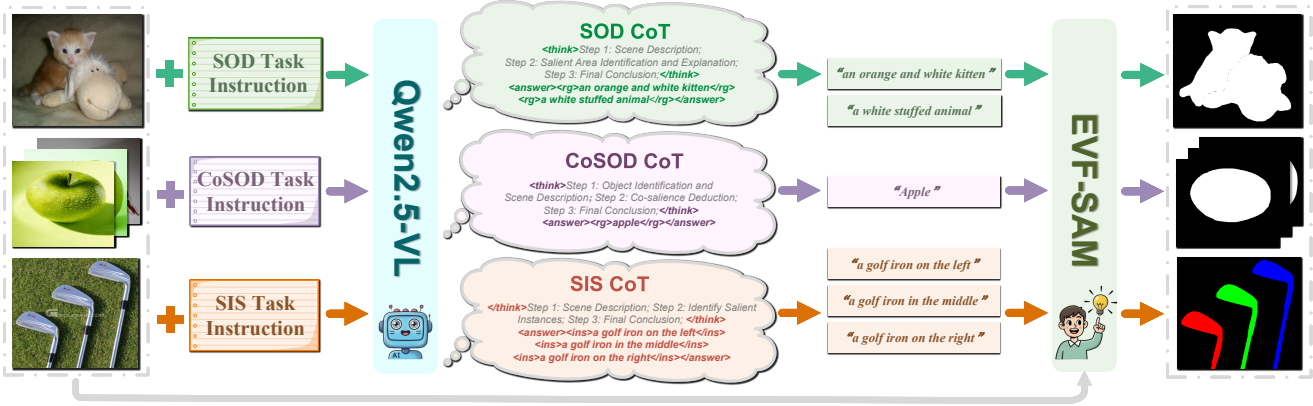


Figure 2. **Overview of the CoT-Saliency framework.** Given visual inputs and task-specific instructions, the VLM (Qwen2.5-vl) generates structured CoT reasoning and referring expressions, which are then parsed and fed into a frozen referring segmentation model (EVF-SAM) to produce task-appropriate masks for SOD, CoSOD, and SIS.

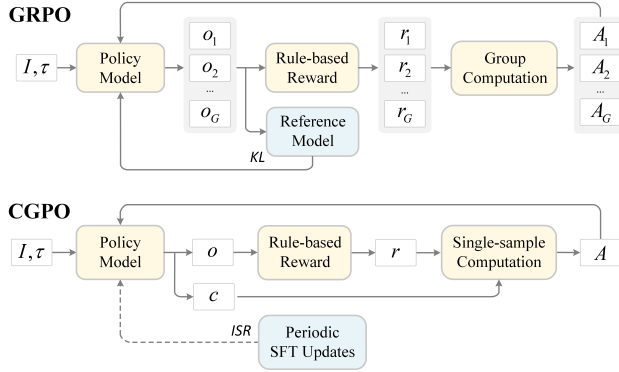


Figure 3. **Comparison between GRPO and our proposed CGPO.** GRPO uses multiple responses per input, group-normalized advantages, and KL regularization with a reference model. CGPO uses a single response, leverages model confidence as a per-sample baseline, and replaces KL with ISR.

parsed from the raw CoT output via simple string matching of the `<answer>` tags.  $\mathcal{E}$  is task-dependent:

$$\mathcal{E} := \begin{cases} \{ \langle \text{rg} \rangle d_i \langle / \text{rg} \rangle \}_{i=1}^N & (\text{SOD}), \\ \langle \text{rg} \rangle [\text{semantic}] s \langle / \text{rg} \rangle & (\text{CoSOD}), \\ \{ \langle \text{ins} \rangle \phi_j \langle / \text{ins} \rangle \}_{j=1}^M & (\text{SIS}). \end{cases} \quad (2)$$

where  $d_i$  is a region description (prefixed by `[semantic]` if categorical),  $s$  is a semantic category, and  $\phi_j$  is a descriptive phrase for instance  $j$  (e.g., “a red cup on the left”). Here,  $N$  and  $M$  denote the number of salient regions for SOD and salient instances for SIS, respectively, with  $i \in \{1, \dots, N\}$  and  $j \in \{1, \dots, M\}$  indexing individual elements.

**Referring segmentation.** Given  $I$  and the parsed  $\mathcal{E} \in \{\mathcal{E}^{\text{SOD}}, \mathcal{E}^{\text{CoSOD}}, \mathcal{E}^{\text{SIS}}\}$ , the segmenter  $\mathcal{S}$  produces the fi-

nal mask(s)  $M$ :

$$M = \begin{cases} \bigvee_{i=1}^N \mathcal{S}(x^{\text{SOD}}, \mathcal{E}_i^{\text{SOD}}) & (\text{SOD}), \\ \{ \mathcal{S}(x_k^{\text{CoSOD}}, \mathcal{E}_k^{\text{CoSOD}}) \}_{k=1}^K & (\text{CoSOD}), \\ \{ \mathcal{S}(x_j^{\text{SIS}}, \mathcal{E}_j^{\text{SIS}}) \}_{j=1}^M & (\text{SIS}), \end{cases} \quad (3)$$

where  $\bigvee$  denotes pixel-wise logical OR (i.e., union) of binary masks, merging all `<rg>` regions into a single salient mask for SOD. This design enables a single frozen  $\mathcal{S}$  (EVF-SAM) to handle all three tasks without architectural modification.

### 3.2. CoT Alignment

We train the VLM to generate high-quality, task-aligned CoT reasoning in two stages. First, Supervised Fine-Tuning (SFT) initializes the model using a curated dataset of ground-truth CoT sequences. Second, Reinforcement Learning (RL) refines the policy with a composite reward that jointly assesses reasoning format and segmentation accuracy (see supplementary material). This encourages structured, task-accurate CoT outputs.

#### 3.2.1. Supervised Fine-Tuning

We curate the SFT dataset using an “output-to-reasoning” strategy. Specifically, we prompt a powerful closed-source world model (i.e., Gemini [6]) with both the input image(s) and the corresponding ground-truth segmentation mask(s), and ask it to explain why the highlighted regions are salient. The resulting CoT explanations are treated as ground-truth reasoning traces for supervised training. This ensures logical consistency between the CoT and the ground-truth masks, while decoupling data quality from the world model’s innate reasoning ability.

The VLM is trained via the standard autoregressive cross-entropy loss to maximize the log-likelihood of the



### SOD Task Instruction

Salient object detection (SOD) aims to identify the visually prominent regions in an image. I will provide an image and ask you to identify its salient regions. Your task is to complete this through step-by-step Chain-of-Thought (CoT) reasoning. Please enclose your CoT and final answer in the tags `<think>` `</think>` and `<answer>` `</answer>`, respectively.

The final answer may contain multiple distinct salient regions, each of which should be described in a simple sentence (or category name) for differentiation. Each description must be enclosed in `<rg>` `</rg>`, and if the description is a category name, it must start with `[semantic]`.



### CoSOD Task Instruction

Co-salient Object Detection (CoSOD) aims to identify salient objects that are common across a group of images. I will provide you with a group of images and ask you to identify the category of co-salient objects within them. Your task is to complete this task through step-by-step Chain-of-Thought (CoT) reasoning. Please enclose your CoT in `<think>` `</think>` tags and your final answer in `<answer>` `</answer>` tags.

The final answer should only include the co-salient category name, enclosed in `<rg>` `</rg>` and starting with `[semantic]`.



### SIS Task Instruction

Salient Instance Segmentation (SIS) aims to identify all prominent instances in an image. I will provide an image and ask you to identify all its salient instances. Your task is to complete this task through step-by-step Chain-of-Thought (CoT) reasoning. Please enclose your CoT and final answer in the tags `<think>` `</think>` and `<answer>` `</answer>`, respectively.

The final answer must include all salient instances, each described in a distinct sentence (e.g., "a {adjective} {classname}" using location or other attributes) for differentiation. Each description must be enclosed in `<ins>` `</ins>`.

Figure 4. Task instruction design for the three saliency tasks.

ground-truth CoT sequences. Formally, for visual input  $I$ , task instruction  $\tau$ , and the corresponding ground-truth CoT response  $o^{\text{gt}} = (o_1^{\text{gt}}, \dots, o_{T^{\text{gt}}}^{\text{gt}})$ , the SFT objective is:

$$\mathcal{J}_{\text{SFT}}(\theta) = \mathbb{E}_{(I, \tau, o^{\text{gt}})} \left[ \sum_{t=1}^{T^{\text{gt}}} \log \pi_{\theta}(o_t^{\text{gt}} | I, \tau, o_{<t}^{\text{gt}}) \right]. \quad (4)$$

Here,  $\pi_{\theta}(\cdot | I, \tau, o_{<t})$  denotes the VLM’s autoregressive policy parameterized by  $\theta$ , *i.e.*, the probability distribution over the next token given the visual input, task instruction, and previously generated tokens.

### 3.2.2. Reinforcement Learning

**Preliminary.** To contextualize our CGPO, we briefly review GRPO [36], a group-based RL algorithm for optimizing autoregressive language policies. For each input pair  $(I, \tau)$ , GRPO samples  $G$  candidate responses  $\{o_i\}_{i=1}^G$ , computes a scalar reward  $r_i \in [0, 1]$  for each, and constructs a group-normalized advantage:

$$A_i = \frac{r_i - \mu_r}{\sigma_r}, \quad (5)$$

where  $\mu_r$  and  $\sigma_r$  are the empirical mean and standard deviation of the  $G$  rewards. The policy update uses the impor-

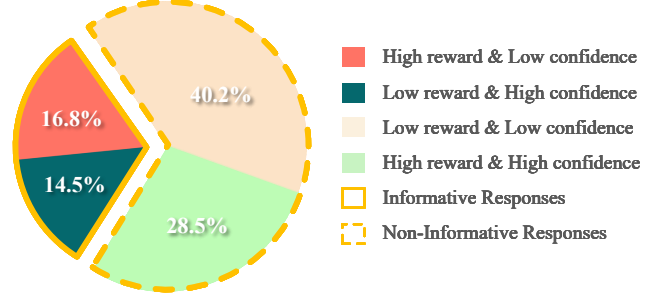


Figure 5. Response type distribution on the SFT-initialized model, categorized by reward and model confidence. We analyze 8,000 responses and define low and high thresholds for both reward and confidence as the bottom 20% and top 20% of their respective empirical distributions. Confidence is calculated as the mean token-wise probability of the generated CoT response.

tance sampling ratio

$$\rho_{i,t}(\theta) = \frac{\pi_{\theta}(o_{i,t} | I, \tau, o_{i,<t})}{\pi_{\theta_{\text{old}}}(o_{i,t} | I, \tau, o_{i,<t})}, \quad (6)$$

combined with a PPO-style clipped objective:

$$\mathcal{C}_i = \frac{1}{T_i} \sum_{t=1}^{T_i} \min(\rho_{i,t}(\theta) A_i, \text{clip}(\rho_{i,t}(\theta), 1 - \varepsilon, 1 + \varepsilon) A_i), \quad (7)$$

and a KL penalty against a fixed reference policy  $\pi_{\text{ref}}$ :

$$\mathcal{L}_i^{\text{GRPO}} = \mathcal{C}_i - \beta D_{\text{KL}}(\pi_{\theta} \| \pi_{\text{ref}}). \quad (8)$$

The overall objective is:

$$\mathcal{J}_{\text{GRPO}}(\theta) = \mathbb{E}_{(I, \tau), \{o_i\}} \left[ \frac{1}{G} \sum_{i=1}^G \mathcal{L}_i^{\text{GRPO}} \right]. \quad (9)$$

**Confidence-Guided Policy Optimization.** Despite its widespread use, GRPO faces three key limitations that impede learning efficiency and policy quality.

First, GRPO is confidence-agnostic: it computes advantages solely from group-level reward statistics and ignores the model’s confidence. By discarding confidence, GRPO fails to focus on informative samples, *i.e.*, high-reward & low-confidence (correct but under-explored) and low-reward & high-confidence (overconfident errors). As shown in Figure 5, these informative responses account for only 31.3% of all samples, while the majority (68.7%) are non-informative (either already well-learned or inherently unreliable). Uniform updates across this imbalanced distribution lead to inefficient learning.

Second, the shared group-mean baseline causes signal dilution. A correct but under-explored response may receive a weakened positive advantage if grouped with already-mastered high-reward samples, while a confidently wrong response may escape strong penalty due to worse outliers.

Third, GRPO incurs prohibitive computational overhead: it requires  $G$  forward passes,  $G$  reward evaluations, and storage of  $G$  KV caches per input due to group sampling, and further adds cost from the KL divergence penalty against a fixed reference model.

To this end, we propose Confidence-Guided Policy Optimization (CGPO), a lightweight single-sample reinforcement learning algorithm that explicitly accounts for the model’s confidence during policy updates to overcome GRPO’s key limitations. Specifically, we reinterpret advantage estimation through a Bayesian lens [18]: the mean token-wise confidence

$$c = \frac{1}{T} \sum_{t=1}^T \pi_{\theta}(o_t \mid \mathbf{I}, \tau, o_{<t}) \quad (10)$$

serves as a proxy for the prior belief that the generated CoT is correct, while the task-specific reward  $r \in [0, 1]$  acts as observational evidence of correctness. The ideal learning signal aligns belief with evidence, a principle known as calibration [7, 32]. Since  $r$  functions as a soft label for correctness [37], the natural misalignment measure is the binary cross-entropy:

$$\mathcal{L}_{\text{NLL}} = -r \log c - (1 - r) \log(1 - c). \quad (11)$$

However, instead of minimizing  $\mathcal{L}_{\text{NLL}}$  directly, we extract a policy update direction from its gradient. Since policy gradient methods maximize an objective, we follow the *negative* gradient of  $\mathcal{L}_{\text{NLL}}$  with respect to  $c$ :

$$-\nabla_c \mathcal{L}_{\text{NLL}} = \frac{r - c}{c(1 - c)}. \quad (12)$$

The numerator  $(r - c)$  captures the discrepancy between reward (evidence) and confidence (prior), *i.e.*, Bayesian surprise [16]. The denominator, however, causes numerical instability near  $c \rightarrow 0$  or  $c \rightarrow 1$ . Discarding this unstable scaling factor, we adopt the signed error  $(r - c)$  as our per-sample advantage:

$$\hat{A} = r - c. \quad (13)$$

This design ensures that high-reward & low-confidence responses receive strong positive advantages, while low-reward & high-confidence ones incur strong penalties; already-aligned samples (high-reward & high-confidence or low-reward & low-confidence) yield near-zero advantages, avoiding unnecessary updates. Crucially, since the baseline  $c$  is computed per-sample from the model’s own confidence, the advantage is free from group interference, eliminating signal dilution, and requires only a single reasoning trace, removing group operations, redundant memory, and computational overhead.

In addition to the single-sample advantage design, we simplify policy regularization by replacing GRPO’s static

KL divergence penalty with **Interleaved SFT Regularization (ISR)**. Specifically, we alternate between RL updates and SFT steps based on the current training step  $s$  and a fixed period  $P$ .

The RL update uses the single-sample advantage and follows a PPO-style clipped objective:

$$\mathcal{J}_{\text{RL}}(\theta) = \mathbb{E}_{(\mathbf{I}, \tau), o} \left[ \frac{1}{T} \sum_{t=1}^T \min \left( \rho_t(\theta) \hat{A}, \text{clip}(\rho_t(\theta), 1 - \varepsilon, 1 + \varepsilon) \hat{A} \right) \right]. \quad (14)$$

The SFT update uses the objective defined in Eq. (4). We alternate between RL and SFT updates every  $P$  steps, yielding the unified objective:

$$\mathcal{J}_{\text{CGPO}}(\theta) = \begin{cases} \mathcal{J}_{\text{RL}}(\theta), & \text{if } s \bmod P \neq 0, \\ \mathcal{J}_{\text{SFT}}(\theta), & \text{if } s \bmod P = 0. \end{cases} \quad (15)$$

## 4. Experiments

### 4.1. Evaluation Datasets and Metrics

We evaluate our unified framework on standard benchmarks for all three tasks: CoSOD (CoCA [61], CoSal2015 [56], CoSOD3k [11]), SOD (DUT-O [52], ECSSD [51], PASCAL-S [25]), and SIS (ILSO [21], SOC [9], SIS10K [35]).

For SOD and CoSOD, we report the Structure-measure ( $S_m$ ) [8], max F-measure ( $F_{\text{max}}$ ) [1], E-measure ( $E_m$ ) [10], and Mean Absolute Error ( $\mathcal{M}$ ) [5]. For SIS, we use standard Average Precision metrics: AP<sub>50</sub>, and AP<sub>70</sub>.

### 4.2. Implementation Details

For SFT data construction, we use *gemini-2.5-pro-preview* [6] to generate CoT annotations conditioned on ground-truth masks, collecting: 1,262 image groups (8 images each) from CoCoSeg [39] for CoSOD, 2,640 images from DUTS-TR [42] for SOD, and 2,467 images from ILSO [21], SIS10K [35], and SOC [9] for SIS. For RL training data, we sample 3,000 examples per task from the same sources.

We base our VLM on Qwen2.5-VL-7B-Instruct [3], freeze its vision encoder, and fine-tune only the language component via LoRA. The downstream segmenter is EVF-SAM-multitask [59]. Training uses AdamW ( $\beta_1 = 0.9$ ,  $\beta_2 = 0.95$ ): 3,000 SFT steps with lr=1e−6, followed by 3,000 CGPO RL steps with lr=1e−4. To stabilize RL without extra cost, we interleave every 3 RL steps with 2 SFT steps. All experiments run on L20 GPUs with PyTorch [33].

### 4.3. Ablation Study

We validate our core contributions through ablation studies on representative datasets: CoCA (CoSOD), ECSSD

Table 1. **Ablation study on key components of our model and training strategy.** We conduct comprehensive ablation experiments on representative datasets from the CoSOD, SOD, and SIS tasks.

Method	CoSOD Task (CoCA)				SOD Task (ECSSD)				SIS Task (ILSO)	
	$S_m \uparrow$	$E_\xi \uparrow$	$F_\beta \uparrow$	$\mathcal{M} \downarrow$	$S_m \uparrow$	$E_\xi \uparrow$	$F_\beta \uparrow$	$\mathcal{M} \downarrow$	MAP@0.7 $\uparrow$	MAP@0.5 $\uparrow$
<i>Ablation Study on RL Algorithm</i>										
○ SFT	0.867	0.910	0.841	0.032	0.890	0.929	0.906	0.046	0.683	0.711
○ SFT+GRPO	0.885	0.935	0.850	0.031	0.895	0.928	0.889	0.049	0.895	<b>0.926</b>
● SFT+CGPO	<b>0.899</b>	<b>0.946</b>	<b>0.871</b>	<b>0.023</b>	<b>0.935</b>	<b>0.968</b>	<b>0.952</b>	<b>0.022</b>	<b>0.902</b>	0.922
<i>Ablation Study for CoT Reasoning</i>										
○ SFT	0.867	0.910	0.841	0.032	0.890	0.929	0.906	0.046	0.683	0.711
○ SFT'	0.890	0.944	0.874	0.026	0.884	0.922	0.902	0.052	0.759	0.787
○ SFT'+CGPO	<b>0.909</b>	<b>0.959</b>	<b>0.902</b>	<b>0.019</b>	0.913	0.951	0.930	0.032	0.864	0.902
● SFT+CGPO	0.899	0.946	0.871	0.023	<b>0.935</b>	<b>0.968</b>	<b>0.952</b>	<b>0.022</b>	<b>0.902</b>	<b>0.922</b>
<i>Comparison with Single-Task Training</i>										
○ SingleTask	0.895	0.945	0.866	0.025	0.925	0.958	0.938	0.027	0.898	0.921
● MultiTask	<b>0.899</b>	<b>0.946</b>	<b>0.871</b>	<b>0.023</b>	<b>0.935</b>	<b>0.968</b>	<b>0.952</b>	<b>0.022</b>	<b>0.902</b>	<b>0.922</b>

(SOD), and ILSO (SIS). Our analysis focuses on three aspects: (1) the effectiveness of our CGPO algorithm over standard GRPO; (2) the necessity of explicit CoT reasoning; and (3) the benefits of joint multi-task training versus task-specific models.

#### 4.3.1. Effectiveness of Proposed RL Strategy

We analyze the impact of our RL strategy. The first row (SFT) in Table 1 shows the model after SFT on our “output-to-reasoning” dataset. The second row (SFT + GRPO) applies the standard GRPO algorithm with  $G = 8$  samples per prompt and a KL-divergence penalty against the SFT checkpoint. The third row (SFT + CGPO) presents our full method, which replaces GRPO’s group-based advantage and KL regularization with a per-sample advantage based on model confidence and ISR.

Results show that CGPO consistently outperforms both SFT and GRPO across all tasks. While GRPO yields modest gains on CoSOD (CoCA) and SIS (ILSO), it degrades performance on SOD (ECSSD), a critical failure highlighting its susceptibility to signal dilution from group normalization. In contrast, CGPO not only avoids this drop but achieves the best results overall (*i.e.*,  $F^\beta = 0.952$  vs. 0.889 on ECSSD).

#### 4.3.2. Effectiveness of CoT Reasoning

To assess the necessity of explicit Chain-of-Thought (CoT) reasoning, we compare four variants in Table 1: (1) SFT: trained on full CoT data; (2) SFT': trained without intermediate reasoning (direct instruction-to-answer mapping); (3) SFT' + CGPO: applies CGPO to the no-CoT model; (4) SFT + CGPO: our full method.

Results show that while the no-CoT model performs well on CoSOD (CoCA), even surpassing SFT, its performance drops sharply on SIS (ILSO), where AP<sub>50</sub> falls from 0.880 to 0.787 (-9.3 pp), underscoring that instance-level

disambiguation requires structured reasoning. RL refinement (SFT' + CGPO) recovers some performance but still lags behind our full model (*e.g.*, AP<sub>50</sub>: 0.902 vs. 0.922 on ILSO;  $F^\beta$ : 0.930 vs. 0.952 on ECSSD).

This task-dependent behavior arises because CoSOD only predicts a single semantic category (*e.g.*, `<rg>[semantic] camera</rg>`), which is easy to learn directly, whereas SOD and SIS require complex, descriptive expressions (*e.g.*, `<ins>a brown dog on the left</ins>`) that benefit from step-by-step reasoning. Our full pipeline achieves the best results on SOD and SIS while remaining competitive on CoSOD, demonstrating that explicit CoT provides a robust inductive bias for unified saliency modeling.

#### 4.3.3. Effectiveness of Joint Multi-Task Training

We compare our unified model against task-specific single-task baselines to assess potential performance trade-offs. As shown in Table 1, the multi-task model achieves on-par or slightly better performance across CoSOD, SOD, and SIS, despite using a single shared architecture.

This suggests strong task compatibility in the shared representation space, with no negative interference. More importantly, our unified model matches or slightly outperforms three separate models while using only one parameter set—offering clear gains in deployment simplicity, memory efficiency, and maintainability.

#### 4.3.4. Training Overhead Comparison

We compare CGPO against two GRPO variants under identical settings (3k RL steps, batch size = 1, H20 GPU). Standard GRPO uses  $G = 8$  reasoning traces per sample and a KL-divergence penalty, consuming 92.4 GB peak GPU memory and 213.8 s per step (Table 2).

Removing KL regularization (“GRPO w/o KL”) while keeping group sampling reduces memory to 72.4 GB and

Table 2. **Training overhead comparison between GRPO and CGPO.** **Traces:** reasoning traces per sample; **Mem:** peak GPU memory; **Step Time:** average training time per step; **Total Time:** wall-clock time for 3k RL steps.

Method	Traces	Mem (GB)	Step Time (s)	Total Time (h)
○ GRPO	8	92.4	213.8	178.2
○ GRPO w/o KL	8	72.4	152.5	127.0
● CGPO	1	38.7	64.7	54.0

step time to 152.5 s, yielding 20% memory savings and 28% speedup by eliminating the reference model’s forward pass.

In contrast, CGPO uses only a single reasoning trace and replaces KL with Interleaved SFT Regularization (ISR), achieving just 38.7 GB memory and 64.7 s per step. Total training time drops from 178.2 h (GRPO) to 54.0 h, a 3.3× speedup, without performance loss.

These results confirm that CGPO eliminates the computational bottlenecks of group sampling and KL regularization, making long CoT alignment both practical and efficient.

#### 4.4. Comparison With State-of-the-Art Methods

We compare our unified framework against recent SOTA methods across SOD, CoSOD, and SIS. As shown in Table 3, our model achieves SOTA or highly competitive performance, despite using only 3,920 training images, far fewer than most competitors (*i.e.*, VST/MENet: 10,553; GCoNet+: 200,000).

In SOD, our method outperforms VST [27], MENet [46], and SelfReformer [55] on all metrics, achieving an S-measure of 0.935 and MAE of 0.022, reflecting superior boundary accuracy and background suppression.

For CoSOD, we surpass strong baselines—including GCoNet+ [62], CONDA [23], DMT+ [22], and VCP [40], with an S-measure of 0.899, a “+8.0 pp” gain over the prior best (VCP: 0.819). This confirms the effectiveness of our CoT-guided cross-image reasoning in identifying true co-salient objects while suppressing distractors.

In SIS, our model outperforms SCNet [34], S4Net [12], RDPNet [49], and OQTR [35] on two of three benchmarks, achieving  $AP_{70} = 0.902$ , demonstrating strong instance disambiguation for overlapping or occluded objects.

These results show that our CoT-based unified framework not only handles operationally heterogeneous tasks in a single model but also matches or exceeds specialized SOTA methods, while being significantly more data-efficient.

#### 4.5. Closed-Source World Model

We compare our framework against five leading closed-source VLMs, Gemini-2.5-Pro, Claude-Sonnet-4.5, GPT-

4o, Qwen-vl-max, Grok-4, and our method, under a fair protocol: for each test sample, we collect their full CoT responses and feed them into our frozen EVF-SAM segmenter to generate masks. Results in Table 5 show our model consistently outperforms all competitors across CoSOD (CoCA), SOD (ECSSD), and SIS (ILSO).

Notably, on SIS (ILSO), our method achieves an  $AP_{50}$  of 0.922, over 24.4 pp higher than the best competitor (Claude-sonet-4-5: 0.678). This gap highlights the limitations of general-purpose VLMs, which, despite their scale, fail to produce the precise, task-specific reasoning needed for saliency tasks in zero-shot settings.

These results validate two key aspects of our approach: (1) our “output-to-reasoning” SFT strategy yields higher-quality CoT than unguided world models, and (2) our CGPO-based RL effectively distills this knowledge into robust reasoning. Together, they demonstrate that a smaller, purpose-built model can surpass larger generalist VLMs in specialized domains.

#### 4.6. Open-Source World Model

We compare our framework against five leading open-source VLMs, Qwen2.5-vl-7b-instruct, Qwen3-vl-32b-thinking, InternVL3-9B, Llava-onevision-qwen2-7b, GLM-4.1V-9B-Thinking, and our method, under a fair protocol: for each test sample, we collect their full CoT responses and feed them into our frozen EVF-SAM segmenter to generate masks. Results in Table 5 show our model consistently outperforms all competitors across CoSOD (CoCA), SOD (ECSSD), and SIS (ILSO).

Notably, on SIS (ILSO), our method achieves an  $AP_{50}$  of 0.922, over 26.7 pp higher than the best competitor (Qwen3-vl-32b-thinking: 0.655). This gap highlights the limitations of general-purpose VLMs, which, despite their scale, fail to produce the precise, task-specific reasoning needed for saliency tasks in zero-shot settings.

These results validate two key aspects of our approach: (1) our “output-to-reasoning” SFT strategy yields higher-quality CoT than unguided world models, and (2) our CGPO-based RL effectively distills this knowledge into robust reasoning. Together, they demonstrate that a smaller, purpose-built model can surpass larger generalist VLMs in specialized domains.

### 5. Conclusion

We present the first unified framework for SOD, CoSOD, and SIS by casting each as a CoT reasoning task in a vision-language model, bridging heterogeneity through a shared CoT interface and frozen segmenter. Our approach combines CGPO, a single-sample RL algorithm using reward–confidence discrepancy as a per-sample advantage, ISR for stable training without KL penalties, and an

Table 3. **Quantitative comparisons with other SOTA methods in conventional SOD, CoSOD and SIS task.** We conduct the comparison on twelve benchmark datasets. We use bold and underline to mark the best and second-best excellent results, respectively.

Salient Object Detection (SOD)														
Methods	Pub.	Training Images	DUT-O[52]				ECSSD[51]				PASCAL-S[25]			
			$S_m \uparrow$	$E_\xi \uparrow$	$F_\beta \uparrow$	$\mathcal{M} \downarrow$	$S_m \uparrow$	$E_\xi \uparrow$	$F_\beta \uparrow$	$\mathcal{M} \downarrow$	$S_m \uparrow$	$E_\xi \uparrow$	$F_\beta \uparrow$	$\mathcal{M} \downarrow$
○ VST [27]	ICCV2021	10553	0.850	0.888	0.800	0.058	0.932	0.964	0.944	0.033	0.873	0.920	0.871	0.060
○ MENet [46]	CVPR2023	10553	0.850	0.879	0.792	<u>0.045</u>	0.928	0.956	0.939	0.031	0.871	0.914	0.872	0.055
○ SelfReformer [55]	TMM2023	10553	0.861	0.894	0.807	<b>0.043</b>	<b>0.936</b>	<u>0.965</u>	<u>0.948</u>	<u>0.027</u>	<u>0.881</u>	<u>0.926</u>	<u>0.883</u>	<u>0.052</u>
● CGPO(Ours)	-	<b>3920</b>	<b>0.864</b>	<b>0.907</b>	<b>0.833</b>	0.049	<u>0.935</u>	<b>0.968</b>	<b>0.952</b>	<b>0.022</b>	<b>0.887</b>	<b>0.935</b>	<b>0.891</b>	<b>0.042</b>
Co-Salient Object Detection (CoSOD)														
Methods	Pub.	Training Images	CoCA[60]				CoSal2015[56]				CoSOD3k[11]			
			$S_m \uparrow$	$E_\xi \uparrow$	$F_\beta \uparrow$	$\mathcal{M} \downarrow$	$S_m \uparrow$	$E_\xi \uparrow$	$F_\beta \uparrow$	$\mathcal{M} \downarrow$	$S_m \uparrow$	$E_\xi \uparrow$	$F_\beta \uparrow$	$\mathcal{M} \downarrow$
○ GCoNet+ [62]	TPAMI2023	208250	0.738	0.814	0.637	0.081	0.881	0.926	0.891	0.055	0.843	0.901	0.834	0.061
○ CONDA [23]	ECCV2024	208250	0.763	0.839	0.685	0.089	0.900	0.938	0.908	0.045	0.862	0.911	0.853	0.056
○ DMT+ [22]	CVPR2023	208250	0.779	0.834	0.689	0.076	0.899	0.935	0.903	0.047	0.866	0.912	0.854	0.054
○ VCP [40]	CVPR2025	208250	<u>0.819</u>	<u>0.871</u>	<u>0.752</u>	<u>0.054</u>	<u>0.927</u>	<u>0.962</u>	<u>0.941</u>	<u>0.030</u>	<u>0.895</u>	<u>0.938</u>	<u>0.893</u>	<u>0.043</u>
● CGPO(Ours)	-	<b>31360</b>	<b>0.899</b>	<b>0.946</b>	<b>0.871</b>	<b>0.023</b>	<b>0.928</b>	<b>0.965</b>	<b>0.942</b>	<b>0.024</b>	<b>0.907</b>	<b>0.950</b>	<b>0.912</b>	<b>0.030</b>
Salient Instance Segmentation (SIS)														
Methods	Pub.	Training Images	ILSO[21]		SIS10K[35]		SOC[9]							
			$AP_{70} \uparrow$	$AP_{50} \uparrow$	$AP_{70} \uparrow$	$AP_{50} \uparrow$	$AP_{70} \uparrow$	$AP_{50} \uparrow$						
○ SCNet [34]	Neurocomputing2020	14207	0.674	0.846	0.692	0.692	0.414	0.609						
○ S4Net [12]	CVPR2019	<b>500</b>	0.636	0.867	0.670	0.833	0.420	0.646						
○ RDPNet [49]	TIP2021	2900	<u>0.885</u>	0.734	0.694	0.820	0.482	0.606						
○ OQTR [35]	TMM2022	9330	0.799	<u>0.904</u>	<u>0.817</u>	<b>0.881</b>	<b>0.725</b>	<b>0.895</b>						
● CGPO(Ours)	-	3920	<b>0.902</b>	<b>0.922</b>	<b>0.843</b>	<u>0.870</u>	0.714	<u>0.745</u>						

Table 4. Comparison experiments of SOTA closed-source models on the ECSSD, CoCA and ILSO datasets.

Method	CoSOD Task (CoCA)				SOD Task (ECSSD)				SIS Task (ILSO)	
	$S_m \uparrow$	$E_\xi \uparrow$	$F_\beta \uparrow$	$\mathcal{M} \downarrow$	$S_m \uparrow$	$E_\xi \uparrow$	$F_\beta \uparrow$	$\mathcal{M} \downarrow$	$MAP_{@0.7} \uparrow$	$MAP_{@0.5} \uparrow$
○ Gemini-2.5-pro	0.832	0.893	0.769	0.045	<u>0.898</u>	<u>0.929</u>	<u>0.894</u>	<u>0.047</u>	0.632	0.673
○ Claude-sonet-4-5	0.880	0.912	0.832	0.026	0.868	0.893	0.855	0.072	<u>0.644</u>	<u>0.678</u>
○ GPT-4o	<b>0.907</b>	<b>0.955</b>	<b>0.885</b>	<b>0.021</b>	0.707	0.727	0.680	0.203	0.529	0.558
○ Qwen-vl-max	0.874	0.904	0.820	0.026	0.823	0.846	0.808	0.108	0.608	0.635
○ Grok-4	<u>0.899</u>	0.944	0.870	<u>0.023</u>	0.790	0.808	0.753	0.116	0.561	0.597
● Ours	<u>0.899</u>	<u>0.946</u>	<u>0.871</u>	<u>0.023</u>	<b>0.935</b>	<b>0.968</b>	<b>0.952</b>	<b>0.022</b>	<b>0.902</b>	<b>0.922</b>

“output-to-reasoning” strategy that ensures logical consistency by prompting a world model to explain ground-truth masks. Despite using far less data, our model matches or exceeds specialized SOTA methods and strong closed-source VLMs, demonstrating that a reasoning-aware, purpose-built architecture achieves superior performance and efficiency.

Table 5.  
**Comparison experiments of SOTA Open-source models on the ECSSD, CoCA and ILSO datasets.**

Method	CoSOD Task (CoCA)				SOD Task (ECSSD)				SIS Task (ILSO)	
	$S_m \uparrow$	$E_\xi \uparrow$	$F_\beta \uparrow$	$\mathcal{M} \downarrow$	$S_m \uparrow$	$E_\xi \uparrow$	$F_\beta \uparrow$	$\mathcal{M} \downarrow$	MAP@0.7 $\uparrow$	MAP@0.5 $\uparrow$
○ Qwen2.5-vl-7b-instruct	0.802	0.837	0.716	0.063	0.518	0.531	0.510	0.372	0.558	0.590
○ Qwen3-vl-32b-thinking	<u>0.881</u>	0.915	<u>0.835</u>	<u>0.026</u>	<u>0.830</u>	<u>0.853</u>	<u>0.814</u>	<u>0.099</u>	<u>0.625</u>	<u>0.655</u>
○ InternVL3-9B	0.830	0.860	0.755	0.045	0.576	0.580	0.559	0.325	0.501	0.545
○ Llava-onevision-qwen2-7b	0.796	0.816	0.792	0.139	0.796	0.816	0.792	0.139	0.456	0.482
○ GLM-4.1V-9B-Thinking	0.858	<u>0.919</u>	0.811	0.037	0.777	0.792	0.762	0.155	0.361	0.414
● Ours	<b>0.899</b>	<b>0.946</b>	<b>0.871</b>	<b>0.023</b>	<b>0.935</b>	<b>0.968</b>	<b>0.952</b>	<b>0.022</b>	<b>0.902</b>	<b>0.922</b>

# CoT-Saliency: Unified Chain-of-Thought Reasoning for Heterogeneous Saliency Tasks

## Supplementary Material

This supplementary material provides additional details and visualizations to support the main paper. Specifically, it includes: (1) qualitative examples of our model’s Chain-of-Thought reasoning and segmentation predictions across the three saliency tasks; (2) the exact prompts used to generate the Supervised Fine-Tuning data via the “output-to-reasoning” strategy; (3) qualitative comparisons with state-of-the-art methods on representative benchmark datasets, illustrating the advantages of our unified CoT-Saliency framework in terms of mask accuracy, instance disambiguation, and robustness to distractors.

### 6. Visualization of Model Predictions

As shown in Figures 6, providing a qualitative visualization of our model’s inference process across the three distinct tasks: Salient Object Detection (SOD), Co-Salient Object Detection (CoSOD), and Salient Instance Segmentation (SIS). A core attribute of our model is its capacity for segmented, step-by-step reasoning. For any given input, the model first generates a textual answer that articulates its analytical process, which then directly informs the generation of the final segmentation mask. This textual output emulates a Chain-of-Thought (CoT) reasoning paradigm, breaking down the complex visual problem into manageable analytical steps.

Crucially, the focus of this reasoning process is dynamically adapted to the specific requirements of each task. For the primary SOD task, the reasoning is centered on modeling intra-image relationships to identify all visually prominent objects within a single image, such as the “orange and white kitten” and the “white stuffed animal”. For the CoSOD task, the model’s reasoning shifts to establishing both inter-image and intra-image relationships to identify the single object category that is common across an entire image group, like the “rubber duck”. Building upon the foundation of SOD, the SIS task further refines this intra-image analysis by compelling the model to not only identify salient objects but also to differentiate between individual instances, as seen with the “grey and white striped kitten” and the “small yellow chick”. The final predicted segmentation masks across all tasks demonstrate high fidelity, characterized by sharp, clean edges that accurately delineate the object contours and align closely with the objects that are perceptually salient to a human observer.

### 7. Prompts for SFT Data Generation

As shown in Figures 7, illustrating the meticulously designed prompts used to generate our Supervised Fine-Tuning (SFT) dataset by querying a large language model (LLM). The fundamental strategy involves providing the LLM with the ground truth (GT)—either the correct object category or the pixel-wise segmentation mask—to guide it in generating high-quality, task-specific reasoning chains. This approach ensures that the generated textual data is both accurate and aligned with the desired analytical framework for each task.

The prompts are engineered with task-specific objectives. For the SOD task, the prompt directs the LLM to identify all visually prominent objects within a single image, emphasizing the contrast and context within that specific scene. For the CoSOD task, the prompt instructs the LLM to analyze an entire group of images to find the common salient object, thereby focusing on the concept of shared visual properties across multiple images. Finally, the prompt for the SIS task requires a more granular level of analysis; building on the principles of SOD, it instructs the LLM to not only identify salient objects but also to distinguish between individual instances by leveraging descriptive attributes such as shape, size, and relative position. This tailored prompt engineering was instrumental in creating a diverse and high-quality dataset for training our model.

### 8. Qualitative Comparison

We compare visual results on CoCA (CoSOD), DUT-O (SOD), and ILSO (SIS). As shown in Figures 8, 9, and 10, our model generates more accurate and complete masks across all tasks.

In CoSOD, our method correctly identifies co-salient objects (*e.g.*, cameras, yellow ducks) and suppresses distractors like humans, while GCoNet+, DMT+, and CONDA often segment irrelevant co-occurring objects. For SOD, our predictions preserve fine details (*e.g.*, climber limbs) with sharp boundaries, whereas MENet and SelfReformer exhibit background leakage or fragmentation. In SIS, our model cleanly separates heavily overlapping instances (*e.g.*, golf clubs), while OQTR and S4Net frequently merge distinct objects.

These results demonstrate that our CoT-guided reasoning significantly improves instance disambiguation and robustness across heterogeneous saliency tasks.



### SOD Task



SOD Task Instruction

</think> ...

#### Step 1: Scene Description

The image shows a close-up view of a small, orange and white kitten sitting on a light-colored, textured surface. The kitten is positioned next to a white, fluffy stuffed animal, which appears to be a sheep or lamb. The kitten is looking directly at the camera.

#### Step 2: Salient Area Identification and Explanation

The salient areas in the image are the kitten and the stuffed animal.

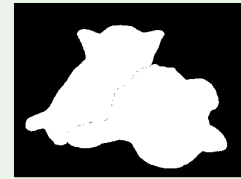
1. Kitten: The kitten is the most prominent object in the scene. It is the main subject, occupying a significant portion of the frame and positioned centrally. Its bright orange and white fur contrasts with the lighter background, and its direct gaze towards the camera naturally draws the viewer's attention. The kitten's facial features and expression also contribute to its saliency.

2. Stuffed Animal: The white stuffed animal, likely a sheep or lamb, is also salient. It is positioned next to the kitten and is in sharp focus. Its fluffy texture and distinct shape make it stand out against the background. Although it is not the main subject, its proximity to the kitten and its own visual characteristics contribute to its saliency.

Both the kitten and the stuffed animal are visually prominent due to their contrast with the background, their central placement, and their inherent interest as subjects (living creature and toy, respectively).

#### Step 3: Final Conclusion

**My final answer regarding salient object detection is:** an orange and white kitten, and a white stuffed animal.</think><answer><rg>an orange and white kitten</rg><rg>a white stuffed animal</rg></answer>.



"an orange and white kitten"

"a white stuffed animal"



### CoSOD Task



CoSOD Task Instruction

</think> ...

#### Step 1: Object Identification:

image1: Contains rubber duck, baby bottle, pacifier, baby rattle, baby teether, baby bib.

image2: Contains rubber duck, bathtub.

image3: Contains rubber duck, bathtub.

image4: Contains rubber duck, towel, table.

image5: Contains cat, rubber duck, toy sofa.

image6: Contains cat, rubber duck, toy sofa.

image7: Contains rubber duck, pool, ladder.

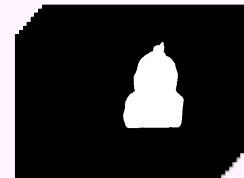
image8: Contains rubber duck, bicycle, flowers, bush.

#### Step 2: Co-saliency Deduction:

By examining the objects identified in each image, we can observe that the object category 'rubber duck' is present in all eight images. While other objects like bathtubs, towels, cats, sofas, pools, and flowers appear in some images, none of these objects are present in all images. The rubber duck is the only object category that is consistently present and often the main subject or a prominent feature across the entire set of images.

#### Step 3: Final Conclusion:

**My final answer regarding co-salient object detection is** rubber duck. </think><answer><rg>[semantic] rubber duck</rg></answer>



"a small cyellow hick sitting next to the kitten"



### SIS Task



SIS Task Instruction

</think> ...

#### Step 1: Scene Description:

The image depicts a close-up scene featuring two small animals, a kitten and a chick, positioned on a textured, woven surface. The background consists of out-of-focus green foliage, creating a shallow depth of field that emphasizes the subjects in the foreground.

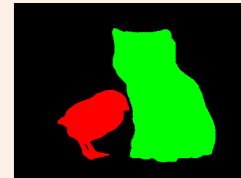
#### Step 2: Identify Salient Instances:

1. The kitten: A grey and white striped kitten is prominently featured in the upper right portion of the image. Its large, expressive eyes and upright posture make it a clear focal point. The sharp focus on the kitten compared to the blurred background further enhances its saliency. Its size relative to the chick and its central placement contribute to its prominence.

2. The chick: A small, yellow chick is located to the left of the kitten, sitting on the woven surface. Its bright yellow color contrasts significantly with the grey kitten and the green background, making it visually distinct. Although smaller than the kitten, its presence alongside the kitten and its clear focus draw attention.

#### Step 3: Final Conclusion

**My final answer regarding salient instance detection is:** a grey and white striped kitten sitting on a woven surface, and a small yellow chick sitting next to the kitten. </think><answer><ins>a grey and white striped kitten sitting on a woven surface</ins> <ins>a small yellow chick sitting next to the kitten</ins></answer>



"a small yellow chick sitting next to the kitten"

"a grey and white striped kitten sitting on a woven surface"

Figure 6. The answer generated by our model and the final segmentation result

## References

- [1] Radhakrishna Achanta, Sheila Hemami, Francisco Estrada, and Sabine Susstrunk. Frequency-tuned salient region detection. In *CVPR*, pages 1597–1604, 2009. 6
- [2] Josh Achiam, Steven Adler, Sandhini Agarwal, Lama Ahmad, Ilge Akkaya, Florencia Leoni Aleman, Diogo Almeida, Janko Altmenschmidt, Sam Altman, Shyamal Anadkat, et al. Gpt-4 technical report. *arXiv preprint arXiv:2303.08774*, 2023. 2
- [3] S. Bai, K. Chen, X. Liu, J. Wang, W. Ge, S. Song, J. Lin, et al. Qwen2. 5-vl technical report. *arXiv preprint arXiv:2502.13923*, 2025. 2, 3, 6
- [4] B. Cheng, I. Misra, A. G. Schwing, A. Kirillov, and R. Girshick. Masked-attention mask transformer for universal image segmentation. In *Proceedings of the IEEE/CVF conference on computer vision and pattern recognition*, pages 1290–1299, 2022. 3
- [5] Ming-Ming Cheng, Jonathan Warrell, Wen-Yan Lin, Shuai Zheng, Vibhav Vineet, and Nigel Crook. Efficient salient region detection with soft image abstraction. In *ICCV*, pages 1529–1536, 2013. 6
- [6] Gheorghe Comanici, Eric Bieber, Mike Schaekermann, Ice Pasupat, Noveen Sachdeva, Inderjit Dhillon, Marcel Blstein, Ori Ram, Dan Zhang, Evan Rosen, et al. Gemini 2.5: Pushing the frontier with advanced reasoning, multimodality, long context, and next generation agentic capabilities. *arXiv preprint arXiv:2507.06261*, 2025. 4, 6
- [7] A Philip Dawid. The well-calibrated bayesian. *Journal of the American statistical Association*, 77(379):605–610, 1982. 2, 6
- [8] Deng-Ping Fan, Ming-Ming Cheng, Yun Liu, Tao Li, and Ali Borji. Structure-measure: A new way to evaluate foreground maps. In *ICCV*, pages 4548–4557, 2017. 6

**Prompt for SFT dataset** **SOD Task**

You are a professional with a deep understanding of the mechanics of human visual attention. Co-salient object detection aims to identify salient objects that are common across a group of images. I will provide you with a **group of images** (they are named `image1`, `image2`, and so on), and the **correct category of co-salient object in the images (ground truth)**. It is known that the co-salient objects in this group of images is `1`, which means that the group's co-salient objects you found are all present in the non-noise images (normal images). Your task is to provide a specific reason explaining the category of co-salient objects in this group of images with **step-by-step Chain-of-Thought (CoT) reasoning**.

In the CoT, the **first step is called 'Object Identification'**, which involves identifying objects in each image. (Notice that you don't care about object properties, just class). The **second step is called 'Co-salience Deduction'**, where you deduce and explain the co-salient object in this group of images. The **third step is called 'Final Conclusion'**, where you arrive at your final answer. Ensuring that your identified co-salient objects are consistent with the gt I provided. (However, please do not mention anything related to 'ground truth' in any of your responses.) Please adhere strictly to the following step titles as specified: **"Step 1: Object Identification," "Step 2: Co-salience Deduction," and "Step 3: Final Conclusion."**

Please note that there may be some noisy images that do not contain a common salient object, but you need to Perform comprehensive object recognition for EACH image in this group (include noise images and normal images) and provide MULTIPLE object categories per image include noise image. When you come to your 'Final conclusion', please ensure that you begin with 'My final answer regarding co-salient object detection is: <co>[semantic]</co>' and end with '</co>', start your task. Ensure that your answers are formatted uniformly each time. (eg. **"My final answer regarding co-salient object detection is: <co>[semantic]</co>"**). Additionally, do not apply any final changes (such as bolding) to the text in the 'Final Conclusion'.

For synonyms like dog and puppy to appear in the object recognition of non-noise images, you can only use one of the words to describe the object. So please use one word to describe the group's co-salient objects for the object recognizes part of all non-noise images. Please start with 'The user is asking for the co-salient object in the provided images. Co-salient object means the object that is salient across all images. I need to look at all the images and identify the object that is present and noticeable in most or all of them,' start your task.

**Prompt for SFT dataset** **CoSOD Task**

You are a professional with a deep understanding of the mechanics of human visual attention. Salient object detection (SOD) aims to identify the visually prominent (i.e., attention-grabbing) regions within an image. I will provide you with an **image and its ground truth mask map**, which highlights the salient areas of the image. Your task is to identify the salient areas in the image through **step-by-step chain-of-thought (CoT) reasoning**, ensuring that your identification of the salient areas is consistent with the salient areas highlighted in the provided ground truth mask.

In the CoT, the **first step is 'Scene Description'**, which involves providing a brief description of the scene depicted in the image. The **second step is 'Salient Area Identification and Explanation'**, which involves identifying which areas are salient and explaining why; this can be accomplished by identifying all objects within the masked areas of the image I provide and describing their characteristics, as well as deducing and explaining why these objects are salient in the image. Please note that when you explain the salience, you should also highlight the contrast relationship of the object to the overall context, as well as its relationship with other objects. Additionally, please explain why some objects are not considered salient (why background objects are background) and analyze the relationship of non-salient objects with the overall context and other objects. The **third step is 'Final Conclusion'**, where you generate a final response that describes the salient areas using concise sentences, please ensure that you begin with 'Final answer: '. Ensuring that the identified salient objects align with the mask image provided. (However, please do not mention anything related to 'ground truth mask map' in any of your responses.) Please adhere strictly to the following step titles as specified: **"Step 1: Scene Description," "Step 2: Salient Area Identification and Explanation," and "Step 3: Final Conclusion"**. Note that the masked areas may consist of sub-regions belonging to different semantic categories. You need to locate each sub-region of the masks in the image using either a single word or a sentence, ensuring that each description is distinct.

When you reach your conclusion, please follow these rules:

1. Use concise text to describe each one, ensuring that each description is distinct and clearly distinguishes each object in the image (e.g., **'a [adjective] [classname]'**) using location or other attributes. Keep responses brief, including category names.
2. For each sub-region, provide a description in one sentence or a single word (preferably a word). Each description should begin with **'<sub>[id]</sub>'**, such as **'Final answer: <sub>[id]</sub> a black cat'**. If you use a single word, please precede it with the **'[semantic]'** tag (e.g., **'Final answer: <sub>[id]</sub> [semantic] person</sub>').** (aiming to minimize the number of sub-region divisions. Please keep the string **'<sub>[id]</sub>'** intact as a whole, without splitting it or adding spaces within it. Additionally, do not include any punctuation marks, such as periods or commas, in the response following 'Final answer: '.
3. If a sub-mask area or the entire mask area contains four or more objects of the same category, use terms like "group" or "several" instead of specifying the exact quantity.
4. Describe each sub-region in plain text.

Please start with 'The user wants me to identify the salient object in the provided image. I need to analyze the input image, try to identify the salient objects within the image and describe each one in a single sentence,' start your task.

**Prompt for SFT dataset** **SIS Task**

You are a professional with a deep understanding of the mechanics of human visual attention. The task of salient instance detection is to identify all salient instances within an image. We will provide you with an **image and a mask image that highlights different salient instances in the original image using distinct colored regions**. Your task is to identify all salient instances in the image by employing **step-by-step Chain-of-Thought (CoT) reasoning**. Please ensure that your responses are consistent with the salient instances highlighted in the provided mask image. (However, please do not mention anything related to 'mask image' or 'masked areas' in any of your responses.)

In the CoT, the **first step is 'Scene Description'**, where you provide a brief description of the scene presented in the image. The **second step is 'Identify Salient Instances'**, which involves identifying the salient instances within the masked areas of the provided image and describing the characteristics of these instances, as well as deducing and explaining why these instances are salient. Please note that when you explain the salience, you should also highlight the relationship of this salient instance to the overall context, as well as its contrast relationship with other instances (whether salient or not). The **third step is 'Final Conclusion'**, where you generate a final response, summarizing each salient instance in a single sentence; please ensure that you begin with 'Final answer: '. Confirm that the salient instances correspond to the masked areas. Please adhere strictly to the following step titles as specified: **"Step 1: Scene Description," "Step 2: Identify Salient Instances," and "Step 3: Final Conclusion"**.

When you reach your conclusion, please follow these rules:

1. For each salient instance, use text to describe each one, ensuring that each description is distinct and clearly distinguishes each instance in the image (e.g., **'a [adjective] [classname]'**) using location or other attributes).
2. Each description should begin with **'<sub>[id]</sub>'**, such as **'<sub>[id]</sub> a black cat on the top'**. Please keep the string **'<sub>[id]</sub>'** intact as a whole, without splitting it or adding spaces within it.
3. If the response after 'Final answer: ' includes multiple categories, each category should begin with **'<sub>[id]</sub>'**, such as **'Final answer: <sub>[id]</sub> a black cat <sub>[id]</sub> a red dog'**. Additionally, do not include any punctuation marks, such as periods or commas, in the response following 'Final answer: '.

Please begin with 'The user wants me to identify the salient instances in the provided image. I need to analyze the input image, try to identify the salient instances within the image and describe it in a single sentence,' directly start your task.

Figure 7. Prompt design for SFT dataset on the three saliency tasks.



Figure 8. Qualitative comparisons with other SOTA CoSOD methods in CoCA dataset.

[9] D. P. Fan, M. M. Cheng, J. J. Liu, S. H. Gao, Q. Hou, and A. Borji. Salient objects in clutter: Bringing salient object detection to the foreground. In *Proceedings of the European conference on computer vision (ECCV)*, pages 186–202, 2018. 6, 9

[10] Deng-Ping Fan, Cheng Gong, Yang Cao, Bo Ren, Ming-Ming Cheng, and Ali Borji. Enhanced-alignment measure for binary foreground map evaluation. In *IJCAI*, pages 698–704, 2018. 6

[11] D. P. Fan, T. Li, Z. Lin, G. P. Ji, D. Zhang, M. M. Cheng, J. Shen, et al. Re-thinking co-salient object detection. *IEEE transactions on pattern analysis and machine intelligence*, 44(8):4339–4354, 2021. 3, 6, 9

[12] R. Fan, M. M. Cheng, Q. Hou, T. J. Mu, J. Wang, and S. M. Hu. S4net: Single stage salient-instance segmentation. In

*Proceedings of the IEEE/CVF conference on computer vision and pattern recognition*, pages 6103–6112, 2019. 2, 3, 8, 9

[13] Daya Guo, Dejian Yang, Haowei Zhang, Junxiao Song, Ruoyu Zhang, Runxin Xu, Qihao Zhu, Shirong Ma, Peiyi Wang, Xiao Bi, et al. Deepseek-r1: Incentivizing reasoning capability in llms via reinforcement learning. *arXiv preprint arXiv:2501.12948*, 2025. 2

[14] Jiahao He, Keren Fu, Xiaohong Liu, and Qijun Zhao. Samba: A unified mamba-based framework for general salient object detection. In *Proceedings of the Computer Vision and Pattern Recognition Conference*, pages 25314–25324, 2025. 3

[15] K. He, G. Gkioxari, P. Dollar, and R. Girshick. Mask r-cnn. In *Proceedings of the IEEE Conference on Computer Vision and Pattern Recognition*, 2017. 2

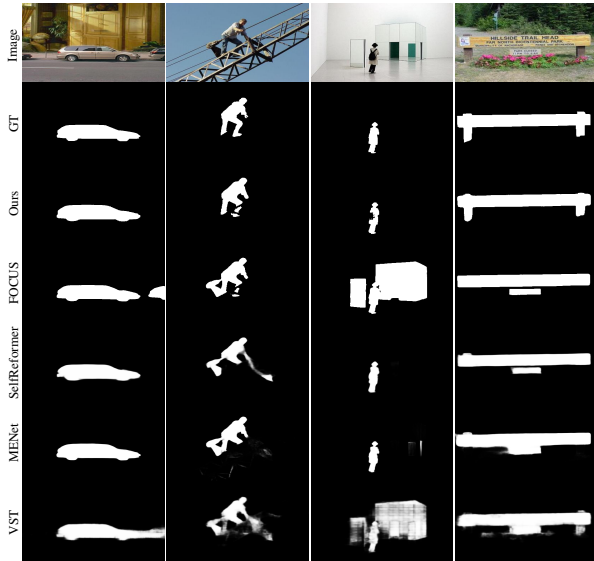


Figure 9. Qualitative comparisons with other SOTA SOD methods in DUT-O dataset.

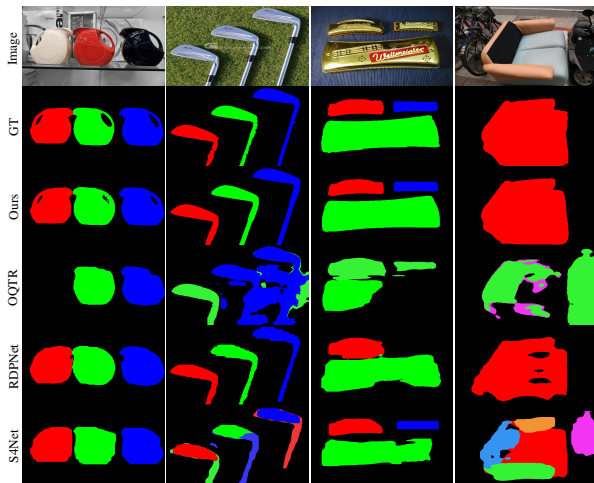


Figure 10. Qualitative comparisons with other SOTA SIS methods in ILSO dataset.

[16] Laurent Itti and Pierre Baldi. Bayesian surprise attracts human attention. *Vision research*, 49(10):1295–1306, 2009. 6

[17] Shiu-hong Kao, Yu-Wing Tai, and Chi-Keung Tang. Think before you segment: High-quality reasoning segmentation with gpt chain of thoughts. *arXiv preprint arXiv:2503.07503*, 2025. 3

[18] Alex Kendall and Yarin Gal. What uncertainties do we need in bayesian deep learning for computer vision? *Advances in neural information processing systems*, 30, 2017. 6

[19] A. Kirillov, E. Mintun, N. Ravi, H. Mao, C. Rolland, L. Gustafson, R. Girshick, et al. Segment anything. In *Proceedings of the IEEE/CVF international conference on computer vision*, pages 4015–4026, 2023. 2, 3

[20] X. Lai, Z. Tian, Y. Chen, Y. Li, Y. Yuan, S. Liu, and J. Jia. Lisa: Reasoning segmentation via large language model. In

*Proceedings of the IEEE/CVF Conference on Computer Vision and Pattern Recognition*, pages 9579–9589, 2024. 3

[21] G. Li, Y. Xie, L. Lin, and Y. Yu. Instance-level salient object segmentation. In *Proceedings of the IEEE conference on computer vision and pattern recognition*, pages 2386–2395, 2017. 3, 6, 9

[22] Long Li, Junwei Han, Ni Zhang, Nian Liu, Salman Khan, Hisham Cholakkal, Rao Muhammad Anwer, and Fahad Shahbaz Khan. Discriminative co-saliency and background mining transformer for co-salient object detection. In *CVPR*, pages 7247–7256, 2023. 8, 9

[23] Long Li, Nian Liu, Dingwen Zhang, Zhongyu Li, Salman Khan, Rao Anwer, Hisham Cholakkal, Junwei Han, and Fahad Shahbaz Khan. Conda: Condensed deep association learning for co-salient object detection. In *European Conference on Computer Vision*, pages 287–303. Springer, 2024. 2, 3, 8, 9

[24] Long Li, Huichao Xie, Nian Liu, Dingwen Zhang, Rao Muhammad Anwer, Hisham Cholakkal, and Junwei Han. Advanced discriminative co-saliency and background mining transformer for co-salient object detection. *IEEE Transactions on Pattern Analysis and Machine Intelligence*, 2025. 2, 3

[25] Yin Li, Xiaodi Hou, Christof Koch, James M Rehg, and Alan L Yuille. The secrets of salient object segmentation. In *CVPR*, pages 280–287, 2014. 6, 9

[26] Nian Liu, Junwei Han, and Ming-Hsuan Yang. Picanet: Learning pixel-wise contextual attention for saliency detection. In *CVPR*, pages 3089–3098, 2018. 2, 3

[27] Nian Liu, Ni Zhang, Kaiyuan Wan, Ling Shao, and Junwei Han. Visual saliency transformer. In *ICCV*, pages 4722–4732, 2021. 2, 3, 8, 9

[28] Yuqi Liu, Bohao Peng, Zhisheng Zhong, Zihao Yue, Fanbin Lu, Bei Yu, and Jiaya Jia. Seg-zero: Reasoning-chain guided segmentation via cognitive reinforcement. *arXiv preprint arXiv:2503.06520*, 2025. 3

[29] Yi Liu et al. Part-object relational visual saliency. *IEEE transactions on pattern analysis and machine intelligence*, 44(7):3688–3704, 2021. 2, 3

[30] Ziyang Luo, Nian Liu, Wangbo Zhao, Xuguang Yang, Dingwen Zhang, Deng-Ping Fan, Fahad Khan, and Junwei Han. Vscope: General visual salient and camouflaged object detection with 2d prompt learning. In *Proceedings of the IEEE/CVF conference on computer vision and pattern recognition*, pages 17169–17180, 2024. 3

[31] Subhabrata Mukherjee, Arindam Mitra, Ganesh Jawahar, Sahaj Agarwal, Hamid Palangi, and Ahmed Awadallah. Orca: Progressive learning from complex explanation traces of gpt-4. *arXiv preprint arXiv:2306.02707*, 2023. 2

[32] Allan H Murphy and Robert L Winkler. Reliability of subjective probability forecasts of precipitation and temperature. *Journal of the Royal Statistical Society Series C: Applied Statistics*, 26(1):41–47, 1977. 2, 6

[33] Adam Paszke, Sam Gross, Francisco Massa, Adam Lerer, James Bradbury, Gregory Chanan, Trevor Killeen, Zeming Lin, Natalia Gimelshein, Luca Antiga, et al. Pytorch: An imperative style, high-performance deep learning library. *NeurIPS*, 32:8026–8037, 2019. 6

- [34] J. Pei, H. Tang, C. Liu, et al. Salient instance segmentation via subitizing and clustering. *Neurocomputing*, 402: 423–436, 2020. 3, 8, 9
- [35] J. Pei, T. Cheng, H. Tang, and C. Chen. Transformer-based efficient salient instance segmentation networks with orientative query. *IEEE Transactions on Multimedia*, 25:1964–1978, 2022. 2, 3, 6, 8, 9
- [36] Z. Shao, P. Wang, Q. Zhu, R. Xu, J. Song, X. Bi, D. Guo, et al. Deepseekmath: Pushing the limits of mathematical reasoning in open language models. *arXiv preprint arXiv:2402.03300*, 2024. 2, 5
- [37] Christian Szegedy, Vincent Vanhoucke, Sergey Ioffe, Jon Shlens, and Zbigniew Wojna. Rethinking the inception architecture for computer vision. In *Proceedings of the IEEE conference on computer vision and pattern recognition*, pages 2818–2826, 2016. 6
- [38] L. Tang, B. Li, S. Kuang, M. Song, and S. Ding. Re-thinking the relations in co-saliency detection. *IEEE Transactions on Circuits and Systems for Video Technology*, 32(8):5453–5466, 2022. 3
- [39] Chong Wang, Zheng-Jun Zha, Dong Liu, and Hongtao Xie. Robust deep co-saliency detection with group semantic. In *AAAI*, pages 8917–8924, 2019. 6
- [40] Jie Wang, Nana Yu, Zihao Zhang, and Yahong Han. Visual consensus prompting for co-salient object detection. In *Proceedings of the Computer Vision and Pattern Recognition Conference*, pages 9591–9600, 2025. 2, 3, 8, 9
- [41] Kunpeng Wang, Zhengzheng Tu, Chenglong Li, Zhengyi Liu, and Bin Luo. Unified-modal salient object detection via adaptive prompt learning. *IEEE Transactions on Circuits and Systems for Video Technology*, 2025. 3
- [42] Lijun Wang, Huchuan Lu, Yifan Wang, Mengyang Feng, Dong Wang, Baocai Yin, and Xiang Ruan. Learning to detect salient objects with image-level supervision. In *CVPR*, pages 136–145, 2017. 6
- [43] Ruiqi Wang and Hao Zhang. Resanything: Attribute prompting for arbitrary referring segmentation. *arXiv preprint arXiv:2505.02867*, 2025. 3
- [44] Song Wang, Gongfan Fang, Lingdong Kong, Xiangtai Li, Jianyun Xu, Sheng Yang, Qiang Li, Jianke Zhu, and Xinchao Wang. Pixelthink: Towards efficient chain-of-pixel reasoning. *arXiv preprint arXiv:2505.23727*, 2025. 3
- [45] X. Wang, T. Kong, C. Shen, Y. Jiang, and L. Li. Solo: Segmenting objects by locations. In *European conference on computer vision*, pages 649–665. Springer, 2020. 3
- [46] Y. Wang, R. Wang, X. Fan, et al. Pixels, regions, and objects: Multiple enhancement for salient object detection. In *Proceedings of the IEEE/CVF conference on computer vision and pattern recognition*, pages 10031–10040, 2023. 8, 9
- [47] Jun Wei, Shuhui Wang, Zhe Wu, Chi Su, Qingming Huang, and Qi Tian. Label decoupling framework for salient object detection. In *CVPR*, pages 13025–13034, 2020. 2, 3
- [48] Jason Wei, Xuezhi Wang, Dale Schuurmans, Maarten Bosma, Fei Xia, Ed Chi, Quoc V Le, Denny Zhou, et al. Chain-of-thought prompting elicits reasoning in large language models. *Advances in neural information processing systems*, 35:24824–24837, 2022. 2
- [49] Yu-Huan Wu, Yun Liu, Le Zhang, Wang Gao, and Ming-Ming Cheng. Regularized densely-connected pyramid network for salient instance segmentation. *IEEE TIP*, 30:3897–3907, 2021. 2, 3, 8, 9
- [50] Can Xu, Qingfeng Sun, Kai Zheng, Xiubo Geng, Pu Zhao, Jiazhan Feng, Chongyang Tao, and Daxin Jiang. Wizardlm: Empowering large language models to follow complex instructions. *arXiv preprint arXiv:2304.12244*, 2023. 2
- [51] Q. Yan, L. Xu, J. Shi, and J. Jia. Hierarchical saliency detection. In *Proceedings of the IEEE conference on computer vision and pattern recognition*, pages 1155–1162, 2013. 6, 9
- [52] C. Yang, L. Zhang, H. Lu, X. Ruan, and M. H. Yang. Saliency detection via graph-based manifold ranking. In *Proceedings of the IEEE conference on computer vision and pattern recognition*, pages 3166–3173, 2013. 6, 9
- [53] Siyue Yu, Jimin Xiao, Bingfeng Zhang, and Eng Gee Lim. Democracy does matter: Comprehensive feature mining for co-salient object detection. In *CVPR*, pages 979–988, 2022. 2, 3
- [54] Yi Ke Yun and Weisi Lin. Selfreformer: Self-refined network with transformer for salient object detection. *arXiv preprint arXiv:2205.11283*, 2022. 2, 3
- [55] Y. K. Yun and W. Lin. Towards a complete and detail-preserved salient object detection. *IEEE Transactions on Multimedia*, 26:4667–4680, 2023. 8, 9
- [56] Dingwen Zhang, Junwei Han, Chao Li, Jingdong Wang, and Xuelong Li. Detection of co-salient objects by looking deep and wide. *IJCV*, 120(2):215–232, 2016. 6, 9
- [57] Jing Zhang, Jianwen Xie, Nick Barnes, and Ping Li. Learning generative vision transformer with energy-based latent space for saliency prediction. *Advances in Neural Information Processing Systems*, 34:15448–15463, 2021. 2, 3
- [58] Ni Zhang, Junwei Han, Nian Liu, and Ling Shao. Summarize and search: Learning consensus-aware dynamic convolution for co-saliency detection. In *ICCV*, 2021. 2, 3
- [59] Yuxuan Zhang, Tianheng Cheng, Lianghui Zhu, Rui Hu, Lei Liu, Heng Liu, Longjin Ran, Xiaoxin Chen, Wenyu Liu, and Xinggang Wang. Evf-sam: Early vision-language fusion for text-prompted segment anything model. *arXiv preprint arXiv:2406.20076*, 2024. 2, 3, 6
- [60] Zhao Zhang, Wenda Jin, Jun Xu, and Ming-Ming Cheng. Gradient-induced co-saliency detection. In *ECCV*, pages 455–472, 2020. 9
- [61] Zhao Zhang, Wenda Jin, Jun Xu, and Ming-Ming Cheng. Gradient-induced co-saliency detection. In *ECCV*, pages 455–472, 2020. 6
- [62] Peng Zheng, Huazhu Fu, Deng-Ping Fan, Qi Fan, Jie Qin, Yu-Wing Tai, Chi-Keung Tang, and Luc Van Gool. Gconet+: A stronger group collaborative co-salient object detector. *IEEE TPAMI*, 2023. 2, 3, 8, 9
- [63] Mingchen Zhuge, Deng-Ping Fan, Nian Liu, Dingwen Zhang, Dong Xu, and Ling Shao. Salient object detection via integrity learning. 2022. 2, 3